Real-time monitoring of the solution growth of ZnO nanorods arrays by quartz microbalances and *in-situ* temperature sensors (Supplementary Information)

Andrea Orsini[a], Christian Falconi[*,a,b]

[a] Department of Electronic Engineering, University of Rome Tor Vergata,

Via del Politecnico 1, 00133, Rome, Italy

[b] CNR IDASC, Via Fosso del Cavaliere, 100, 00133 Rome, Italy

To whom correspondence should be addressed: falconi@eln.uniroma2.it

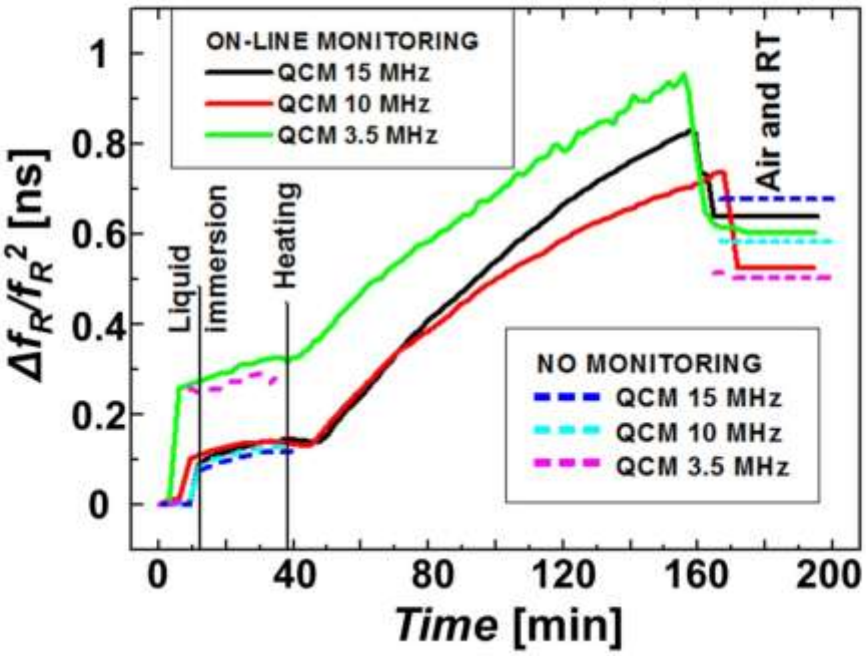

Figure S1. Experiments for ruling out the presence of artifacts. Comparison among the normalized resonant frequency variations of quartzes with different resonant frequencies, with or without on-line monitoring, with temperature equal to 90 °C and equimolar 2.5 mM concentration of zinc nitrate and HMTA; the final values are taken in air and at room temperature (RT).

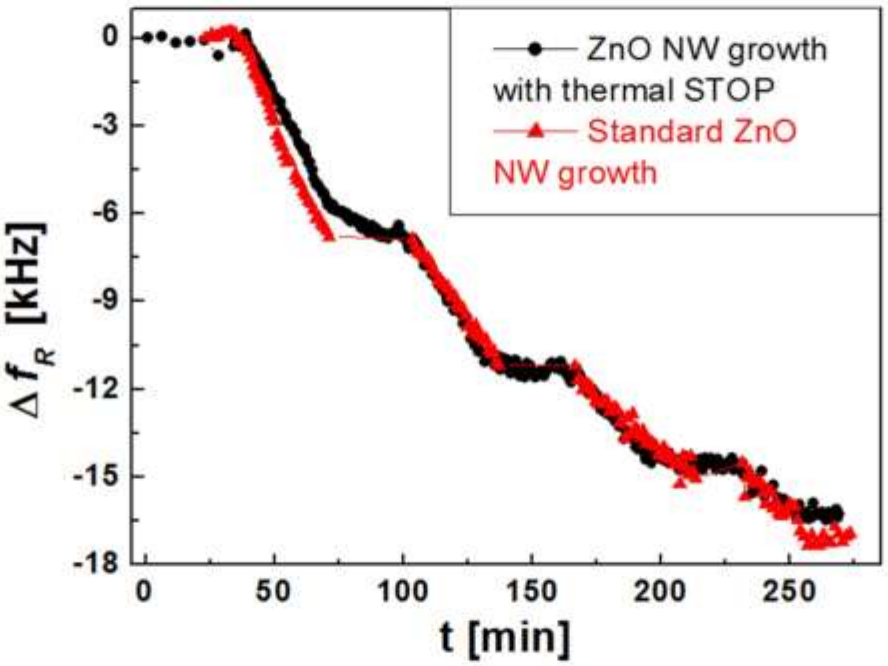

Figure S2. Comparison between growth with thermal interruption and standard growth.

Variations of the resonant frequencies for quartzes with initial resonant frequency 3.579 MHz, at 90°C and with 5mM equimolar concentrations of zinc nitrate and HMTA; the comparison between the growth with interruptions induced by thermal cycles (black circles) and the standard growth (red triangles) shows that the growth rate is only very weakly modified by thermal interruptions.

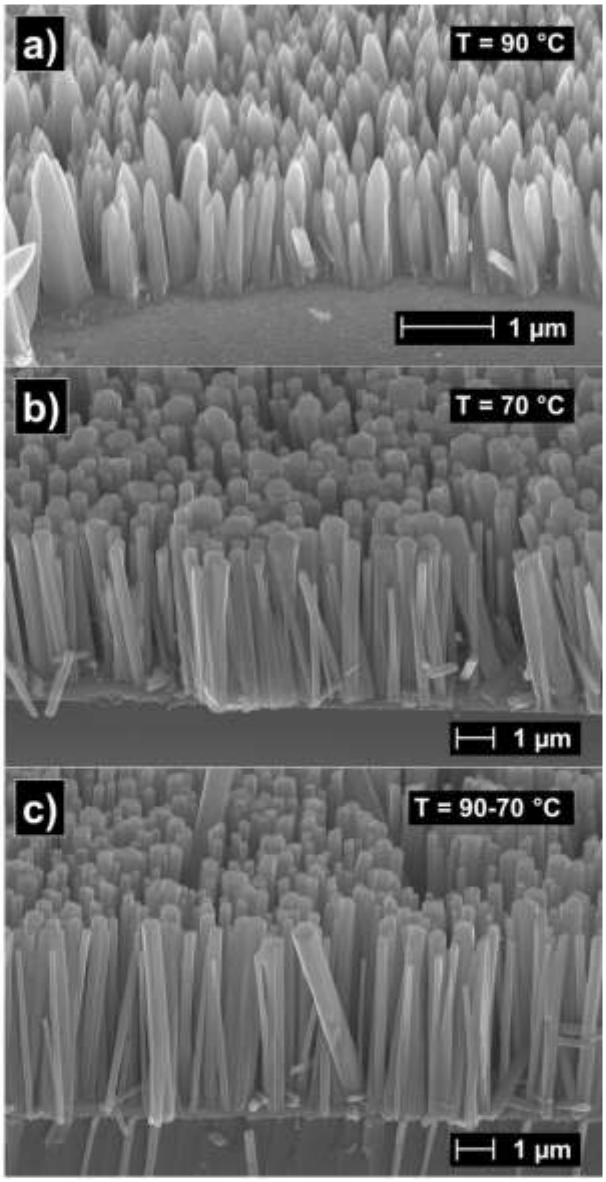

Figure S3. SEM images of ZnO nanorods grown on gold thin films without on-line monitoring. SEM images (45° tilted view) of ZnO nanorods grown on a gold thin film deposited on a silicon substrate with growth time equal to 40 hours, 2.5mM equimolar concentrations of zinc nitrate and HMTA, at 90 °C (a); 70 °C (b) and 90-70 °C (c).

Supplementary Discussion

1. Electro-mechanical resonators in liquids

Electro-mechanical resonators are often employed for monitoring vacuum thin-film deposition techniques; in practice, quartz crystals are the most widely used electromechanical resonators because of their very small electro-mechanical losses (*i.e.* high Q resonators), low cost, high purity, rare crystal imperfections, and availability of temperature-compensated and stress-compensated cuts. For small mass loading Δm, the variation Δf_m of the quartz resonant frequency in air can be described by the Sauerbrey equation [1]:

$$\Delta f_m = \frac{-2 f_{R,IN}^2 \Delta m}{S\sqrt{\mu_Q \rho_Q}} \tag{1}$$

where $f_{R,IN}$ is the initial resonant frequency, S is the piezoelectric active area, μ_Q and ρ_Q are the shear stiffness and the mass density of the quartz, respectively; the quartz can also be modeled by the simple Butterworth-Van Dyke model, *i.e.* a series resonant RLC circuit with a parallel capacitance. Though widely used, quartzes in liquids are worse than in vacuum or in air because liquids generally introduce significant losses and, therefore, reduce the quality factor of the resonance; moreover, the resonant frequency in liquids depends on mass variation but also on the viscous coupling with the liquid, surface roughness, surface stresses, and both the liquid conductance and dielectric constant [2,3], with the liquid conductance being especially critical when both the electrodes are exposed to the same solution (as, in such cases, the liquid introduces a parasitic conductance in parallel to the resonator). Quartz oscillations in liquids have been investigated by Kanazawa *et al.* [4] who found that the variation of the resonant frequency of a thickness shear mode resonator induced by liquid loading can be approximated as

$$\Delta f_L = -f_R^{3/2}\sqrt{\frac{\eta_L \rho_L}{\pi \mu_Q \rho_Q}} \tag{2}$$

where ρ_L and η_L are the liquid density and shear viscosity. Subsequently, many studies have been performed on monitoring of thin films deposition in liquids [5–8], including in electrochemistry, where one of the quartz electrodes can also be used as a working electrode for electrodeposition. In our experiments we verified that the effect of the liquid loading on the total frequency shift is not accurately predictable, most likely due to the dependence of the liquid loading on the roughness of the surface which, clearly, is affected by the growth of nanowires. However, by considering many experiments, we computed the ratios between the frequency shift found in-liquid and the frequency shift measured in air, after emersion of the quartz; these ratios were comprised between 1.1 and 1.25, *i.e.* the additional frequency shift due to the liquid loading is between 10% and 25% of the frequency resonant shift in air. Therefore, if we consider an average liquid contribution equal to 17.5% of the frequency resonant shift in air, we may easily extract, from on-line in-liquid measurements, reasonable estimations (±7.5% error) of the resonant frequency shift in air, which is related to the total nanowires deposited-mass by the Sauerbrey Eq. (1).

2. Ruling out artifacts

The proposed on-line monitoring strategy is very unlikely to introduce artifacts. In fact, first, even in oscillating quartzes the amplitude of motion is extremely small (*e.g.* smaller than the lattice constants) and, second, the amplitude of motion of a quartz connected to a network analyzer is even smaller (because, in contrast with an oscillator, the network analyzer does not significantly excite the resonance of the quartz). However, we have performed additional experiments in order to rule out the unlikely presence of artifacts originated by on-line monitoring. In practice, after the end of the deposition, *i.e.* in air and at room temperature, we can consider the Sauerbrey Eq. (1) as a quantitative measure of the total deposited mass. Therefore, we have used quartzes with different initial resonant frequencies as substrates for the growth of ZnO nanorods, with or without on-line monitoring. Since all the quartzes have the same density, shear modulus, and piezoelectric active area, from Eq. (1), the total mass variations are expected to be proportional to $-\Delta f_R / f_R^2$. Therefore, Fig. S1 demonstrates that, with or without on-line monitoring, there is no detectable difference in the mass deposition per unit area among quartzes with different resonant frequencies, with and without monitoring (*i.e.* the spread in the deposited mass is larger than the difference between the cases with and without monitoring); SEM images also confirm that there is no detectable differences in samples obtained with or without on-line monitoring.

3. Electronic interface

The electronic interface [9] for electro-mechanical resonators under vacuum or in air may simply be a standard oscillator circuit [10,11]; however, in liquids, the reduced quality factor may complicate the electronic interface design [2,3,12–14]; in our case this problem is exacerbated by the growth of nanostructures, which further degrades the quality factor. Therefore, for maximum accuracy and simplicity, we preferred to measure the admittance of the resonator by means of a conventional network analyzer.

3. Growth with thermal interruptions

Figure S2 shows the comparison between a growth with interruptions induced by thermal cycles (temperature cycling between 25 °C and 92 °C) and a standard (i.e. with constant temperature, 92 °C, and no interruptions) growth where, for the sake of comparison, the standard growth has been modified for simulating "ideal" interruptions *(i.e.* we have included dummy-data points which artificially and ideally interrupt the reduction of f_R so that the two growth rates are easily comparable); as evident, the growth rate is only very weakly modified by the thermal interruptions.

4. Un-monitored growth on gold thin films

In order to explore the applicability of our dynamic-temperature process to non-resonating substrates and without on-line monitoring, we have grown arrays of ZnO nanorods on different substrates. In order to repeat the growth of a dense array of ZnO nanorods on substrates different from the packaged quartz resonators, we induced a galvanically assisted growth by attaching with silver paste an iron wire to the gold surface. In fact, the high density growth of ZnO nanostructures onto the QCM silver electrode is due to the galvanic effect induced by the electrical contact with the metallic package in solution [15] as recently proposed by another research group [16]. Therefore, we repeated the experiments, with 2.5 mM equimolar concentrations of zinc nitrate and HMTA, in a standard borosilicate bottle with 250 mL volume of solution with different substrates, namely gold-coated silicon, with an intermediate titanium adhesive layer. We prepared three distinct samples of equal area (about 0.5 cm^2), each one in a different bottle filled with the nutrient solution. We prepared two thermostated hot water baths with two different water temperatures, 90 °C and 70 °C. Then, we immerged two bottles in the bath at higher temperature (90 °C) and one in the bath at lower temperature (70 °C). After 36 minutes from the beginning of the experiment (*i.e.* approximately the time where the derivatives of the resonant frequencies obtained in the constant-temperatures experiments, 90 °C and 70 °C, intersect in our previous experiment, see Fig. 3(b) in the main text), we moved one of the bottle from the water bath at 90 °C to the water bath at 70 °C. We interrupted the experiment after 40 hours. As shown in Fig. S3, there is a clear increase of the length of the ZnO nanorods from Fig. S3(a) (experiment at 90 °C), where the rods are in the range of 1.5 – 2 μm, to Fig. S3(b) (experiment at 70 °C), where the rods are in the range 5.5 – 6 μm, to Fig. S3(c) (dynamic 90 °C – 70 °C temperature growth), where the rods are in the range 6.7 – 7.2 μm.

References

1. Mecea, V. M. Is quartz crystal microbalance really a mass sensor? *Sens. Actuators A* **128,** 270–277 (2006).

2. Eichelbaum, F., Rsler, S., Auge, J. & Hauptmann, P. Quartz crystal microbalance sensor in liquids. *Sens. Actuators B Chem.* **19**, 518–522 (1994).

3. Borngräber, R., Schröder, J., Lucklum, R. & Hauptmann, P. Is an oscillator-based measurement adequate in a liquid environment? *IEEE Trans. Ultrason. Ferroelectr. Freq. Control*, **49***,* 1254–1259 (2002).

4. Kanazawa, K. K. & Gordon II, J. G. Frequency of a Quartz Microbalance in Contact with Liquid. *Anal. Chem.* **57***,* 1771–1772 (1985).

5. Murase, K., Tada, H., Shinagawa, T., Izaki, M. & Awakura, Y. QCM Studies of Chemical Solution Deposition of ZnO. *J. Electrochem. Soc.* **153***,* 735–740 (2006).

6. Buttry, D. A. & Ward, M. D. Measurement of Interfacial Processes at Electrode Surfaces with the Electrochemical Quartz Crystal Microbalance. *Chem. Rev.* **92***,* 1355–1379 (1992).

7. Reyes, P. I., Zhang, Z., Chen, H., Duan, Z., Zhong, J., Saraf, G., Lu, Y., Taratula, O., Galoppini, E. & Boustany, N. N. A ZnO Nanostructure-Based Quartz Crystal Microbalance Device for Biochemical Sensing. *IEEE Sens. J.* **9***,* 1302–1307 (2009).

8. Zaera, F. Probing liquid/solid interfaces at the molecular level. *Chem. Rev.* **112***,* 2920–2986 (2012).

9. Falconi, C., Martinelli, E., Di Natale, C., D'Amico, A., Maloberti, F., Malcovati, P., Baschirotto, A., Stornelli, V. & Ferri, G. Electronic interfaces. *Sens. Actuators B* **121***,* 295–329 (2007).

10. Vittoz, E. A., Degrauwe, M. G. R. & Bitz, S. High-performance crystal oscillator circuits: theory and application. *IEEE J. Solid-State Circuits* **23***,* 774–783 (1988).

11. Falconi, C., Massari, A. & D'Amico, A. PTAT oscillators for low Q resonating sensors. *Sens. Actuators B 113,* 120–126 (2006).

12. Nakamoto, T. & Kobayashi, T. Circuit for measuring both Q variation and resonant frequency shift of quartz crystal microbalance. *IEEE Trans. Ultrason., Ferroelectr., Freq. Control* **41***,* 806–811 (1994).

13. Arnau, A., Sogorb, T. & Jiménez, Y. A new method for continuous monitoring of series resonance frequency and simple determination of motional impedance parameters for loaded quartz-crystal resonators. *IEEE Trans. Ultrason., Ferroelectr., Freq. Control* **48***,* 617–623 (2001).

14. Rodahl, M. & Kasemo, B. A simple setup to simultaneously measure the resonant frequency and the absolute dissipation factor of a quartz crystal microbalance. *Rev. Sci. Instrum.* **1996**, *67,* 3238–3241.

15. Scarpellini, D., Paoloni, S., Medaglia, P. G., Pizzoferrato, R., Orsini, A. & Falconi, C. Structural and optical properties of dense vertically aligned ZnO nanorods grown onto silver or gold thin films by galvanic effect with iron contamination. *Submitted to Mater. Sci. Eng. B*

16. Zheng, Z., Lim, Z. S., Peng, Y., You, L., Chen, L. & Wang, J. General Route to ZnO Nanorod Arrays on Conducting Substrates via Galvanic-cell-based approach. *Sci. Rep.* **2013**, *3*, 2434.